npj | heritage science

Article

https://doi.org/10.1038/s40494-025-01779-8

Exploring the spatial interplay between hydro-climatic extremes and armed conflicts in history

Check for updates

Chenyao Jiang[1,2], Will W. Qiang[1,2] & Harry F. Lee[1] ✉

The Taiping Rebellion (1851–1864), the deadliest civil war in Chinese history, has been studied for its societal and climatic links, while its spatial dynamics remain underexplored. This study quantifies the spatial relationship between hydro-climatic extremes and armed conflict during the rebellion. Using panel Poisson fixed-effects estimation, we examine how droughts and floods influence the conflict occurrence both locally and in surrounding areas, applying buffer zones of 10 km, 25 km, 50 km, and 100 km. We cross-validate results using both Qing administrative boundaries and 100 km × 100 km grid-based spatial data. Our findings show that floods, more than droughts, significantly increase the likelihood of local armed conflicts, with the strongest correlation found within a 10 km radius. This spatial pattern may reflect the limited mobility of displaced populations in late Qing China. The study underscores the importance of spatial context in understanding climate-driven conflict risks in vulnerable regions.

The relationship between climate change and collective violence has been a longstanding scholarly debate. Numerous large-N quantitative studies have explored the effects of extreme hydro-climatic events on violent conflicts, particularly in agricultural societies in Africa[1–6] and Central-East Asia[7–11]. Some studies of past societies have also revealed this effect[12–15]. These studies often follow a causal model of "climate deterioration—crop failure—social instability" to explain the link between climate change and violent conflicts. In China, extended periods of cooling are widely considered to have contributed to the fall of dynasties[16–20]. Severe droughts have been linked to the collapse of civilizations such as the Mayans and the Roman Empire[21–24]. However, broad historical analyses often overlook regional variations and the specific impacts of short-term climatic extremes, such as floods and droughts, on conflict emergence. Investigating particular historical events can provide deeper insights into the mechanisms through which climate, ecosystems, and human societies interact[25].

Chinese history has witnessed numerous instances of social upheaval, particularly peasant rebellions[26]. Peasant revolts in agrarian societies are always attributed to irrational agricultural structures and distributional practices that created an organized proletariat against an economically weak and politically rigid upper class, ultimately leading to revolutionary wars[27,28]. Climate plays more of a triggering role in this, with harsh climatic conditions increasing the frequency of wars through food shortages, resulting in social instability and increased violent competition for resources[15,19,29,30]. The Taiping Rebellion (1851–1864) was one of the deadliest civil wars in history[31–34], lasting 14 years and affecting 18 provinces, including the wealthy Jiangnan region[35]. Some estimates suggest a population decline of up to 100 million, nearly a quarter of the nation's population[36]. Historical climatologists have highlighted the catastrophic floods of 1823 in Jiangsu and Zhejiang provinces, which severely impacted agricultural output in the Yangtze River basin, contributing to the economic decline of the Qing Dynasty and setting the stage for the rebellion[17,35,37]. Additionally, Ge and Wang[38] identified a cooling trend in nineteenth-century China, accompanied by increased floods and other extreme weather events. In Guangxi, the Taiping Rebellion's origin, agricultural failures from 1830 to 1850 were particularly severe, with at least 10 years of poor harvests[39]. Low temperatures and flooding further diminished yields, exacerbating human-land conflicts during the Qing Dynasty[15,37,38]. Quantitative studies by Lee et al.[14] suggest that floods had a more significant impact than droughts on civil unrest in the rice-producing areas affected by the rebellion. Similarly, there exists a positive correlation between violent conflict frequency and droughts and floods in the North China Plain during the nineteenth century[40].

Despite previous work on the climate-conflict nexus during the Taiping Rebellion, most studies remain qualitative, with quantitative analyses being notably rare. Existing quantitative research predominantly consists of correlation analyses by establishing time series of socio-economic indicators, conflicts, and climate variations (like temperature or precipitation)[12,15,38], neglecting key spatial dimensions. For example, Ge and Wang established a correlation between the failure curves from 1730 to 1910

[1]Department of Geography and Resource Management, The Chinese University of Hong Kong, Shatin, New Territories, Hong Kong SAR, China. [2]These authors contributed equally: Chenyao Jiang, Will W. Qiang. ✉e-mail: harrylee@cuhk.edu.hk

and the sequence of climatic hazards from 1470 to 1949 to illustrate that the Taiping Rebellion was driven by large-scale annual failures in agricultural production across the country induced by climate change[38]. Zhang et al. constructed a correlation between temperature and harvest and found that the Taiping Rebellion erupted when harvests fell to a critical point during the cold period[15]. Specifically, there has been little investigation into: (1) how varying intensities of droughts and floods differentially affect violent conflicts across space, and (2) whether neighboring regions experiencing such climatic extremes are similarly impacted, and to what extent. These gaps have left the spatial correlation between hydro-climatic extremes and violent conflicts insufficiently explored.

To fill this gap, we selected the regions affected by the Taiping Rebellion (1851–1864) as the study area. We collected data on all the armed conflicts between the Taiping Army and the Qing government forces[41], as well as hydroclimatic extremes (including floods and droughts at different levels) data from 40 meteorological stations in this study area[42]. This study employs the panel Poisson fixed-effects estimation to analyze the spatial dynamics of the droughts/floods-conflict nexus during the Taiping Rebellion. We validate our findings using Qing administrative division (prefecture) data and a 100 km × 100 km grid-based dataset. Buffer zones of 25 km, 50 km, and 100 km are used to assess the influence of climatic disasters on violence in adjacent regions. These insights aim to clarify the spatial dynamics of climate-related conflict in both historical and contemporary contexts.

Methods

Research context

In the mid-nineteenth century, the Qing Dynasty faced over a hundred anti-Qing insurrections across various regions of China[43]. The resistance was particularly pronounced in the provinces of Guangxi, Guangdong, and Hunan, with Guangxi, where the Qing authority was weakest, emerging as the epicenter of resistance. In the summer of 1850, a severe famine struck Guangxi, which the leaders of the Taiping Rebellion perceived as an opportune moment to mobilize their forces. On 11 January 1851, Hong Xiuquan and his followers initiated the rebellion in Jintian village, establishing the "Taiping Tianguo" regime. Following the Jintian Uprising, the Taiping Army rapidly expanded, capturing Dahuangjiangkou (modern-day Jiangkou Town, Guangxi Province) and subsequently extending its control to cities in Guangxi, Hunan, Hubei, Wuchang, Anhui, and Jiangsu. Their influence further reached Henan, Shanxi, and Hebei. Simultaneously, peasant uprisings in northern China, including the Nien Rebellion (1851–1868), frequently erupted in the Yellow and Huaihe River Basins[44]. These widespread revolts affected key provinces and economic centers across China. Accordingly, this study focuses on the 16 provinces of China Proper affected by the Taiping Rebellion, shown in Fig. 1.

The temporal scope of this research is confined to the period of the Taiping Rebellion, specifically 1851–1864. By the mid-nineteenth century, the population of the Qing Dynasty had nearly tripled compared to the preceding century, placing immense pressure on the limited arable land. Between 1753 and 1842, per capita farmland decreased by 78% in the eight provinces where the Taiping and Nien armies operated[38]. Concurrently, significant hydro-climatic anomalies were observed at both regional and global levels[21,45,46]. A marked shift toward colder temperatures, coupled with extreme hydrological events such as droughts and floods, led to widespread agricultural failures, exacerbating the already intense competition for land and resources[26,47,48]. The issue of unequal farmland distribution further compounded these challenges. Government-owned land accounted for approximately one-tenth of the total arable land. At the same time, peasants, who constituted most of the population, relied on only 30–40% of the land for subsistence[38]. Additionally, tenants were prohibited from owning land and were forced to lease fields annually, often purchasing seeds at exorbitant prices from landowners while being compelled to sell their grain at reduced prices in the autumn[49]. Consequently, these populations experienced chronic food insecurity and material deprivation, even during periods of favorable agricultural yields, with their circumstances deteriorating markedly during episodes of harvest failure.

The synergy of social tensions and adverse climatic conditions during this period created fertile ground for peasant revolts. Therefore, the Taiping Rebellion is a valuable case study for analyzing the complex interplay between climate, society, and violent conflicts.

Data collection

To ensure data reliability, this study utilizes well-established climate and socio-economic datasets from prior research:

Data on armed conflicts are drawn from the *Tabulation of Wars in Historical China*, which records detailed information about Chinese wars from 800 B.C. to A.D. 1911[41]. This dataset offers a distinct advantage over other databases due to its inclusion of detailed geographical information about each conflict, which is crucial for spatial analysis. This study focuses on the armed conflicts between the Taiping Army and Qing government forces during 1851–1864. The Taiping Rebellion spanned a long period and affected many regions throughout the country. To better understand the dynamics of the rebellion, we calculated the centroids of the regions where conflicts occurred, weighted by the annual frequency of conflicts, and analyzed their travel routes (Fig. 2).

In the early phases of the rebellion, the Taiping army experienced rapid expansion northward from its point of origin in Guangxi, achieving its northernmost extent in 1853 when it entered Anhui. During the Taiping Rebellion, which lasted from 1850 to 1864, there were three significant southward retreats of conflict centroids in 1854, 1857, and 1859. Notably, 1859 marked the furthest southward advance and signaled the beginning of the decline of the rebellion. In the later stages of the rebellion, spanning from 1860 to 1864, the conflict centroids hovered in three provinces of East China (Jiangsu, Zhejiang, and Anhui), where the Taiping and Qing armies engaged in a series of significant conflicts centered around Nanjing, the capital established by the Taiping forces (also the capital of Jiangsu province). In 1864, the conflict centroids moved westward due to Qing armies pursuing the remnants of the Taiping forces in Sichuan, Hubei, and other regions.

Hydro-climatic extremes are events that deviate significantly from average conditions due to climate change disrupting the hydrologic cycle[50]. In this study, we consider recorded anomalous hydrological events, such as droughts and floods, as hydrological anomalies resulting from climate change, as these events deviate from the norm and attract societal attention. Our data on hydro-climatic extremes are sourced from the *Yearly Charts of Dryness/Wetness in China for the Last 500-year Period*[42], as well as the *Yearly Charts of Dryness/Wetness in NW China for the Last 500-year Period (1470–2008)*[51]. Using a 5-point grading scale (from grade 1 to grade 5 to indicate the range from extreme floods to extreme droughts), the former provides hydro-climatic extremes sequences for 120 locations across China from 1470 to 1979, while the latter revises the sequences for 12 sites in northwestern China and adds grade sequences for seven additional locations. This study integrates these two datasets and selects the 40 metrological stations within the study area to identify occurrences of floods (grades 1 and 2) and droughts (grades 4 and 5).

We calculate the number of sites experiencing extreme floods (grade 1), normal floods (grade 2), normal droughts (grade 4), and extreme droughts (grade 5) each year[52] and employ Kriging interpolation to reveal the wet-dry pattern of the study area during Taiping Rebellion (Fig. 3). In the early years of the Taiping Rebellion (1851–1855), the region predominantly experienced humid conditions, with the conflict centroids all located within more humid areas. From 1856 to 1859, a discernible shift towards drier climatic conditions occurred, accompanied by two significant southward retreats of the conflict's center of mass. Starting in 1860, the differentiation between wet and dry patterns became increasingly indistinct while the rebellion gradually ended.

Panel Poisson fixed-effects estimation

The panel Poisson fixed-effects estimation provides a robust method for analyzing historical armed conflict data, particularly when many observations are zero[53]. During the Taiping Rebellion (1851–1864), many regions remained unaffected and experienced no armed conflicts, resulting in

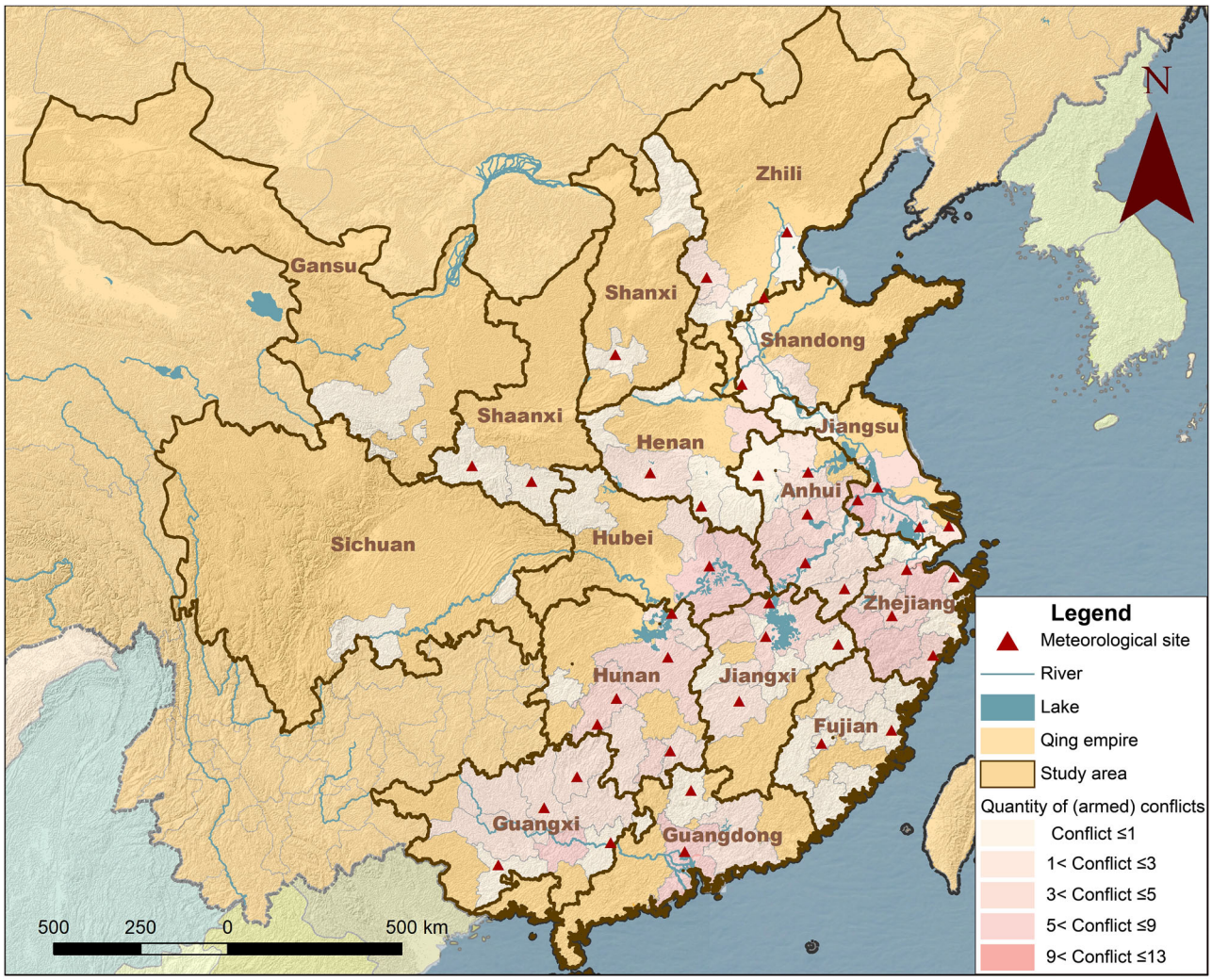

Fig. 1 | Provinces and prefectures that had armed conflicts pertinent to the Taiping Rebellion. The red triangles represent meteorological stations that recorded hydro-climatic extremes. The peach-colored areas indicate the number of armed conflicts within each prefecture.

numerous zero values in the dataset. This sparse distribution makes standard linear regression and ordinary Poisson regression less reliable, as they can produce unstable or biased results when applied to such data. The panel Poisson fixed-effects estimation, however, effectively addresses these challenges.

Unlike traditional Poisson regression, which assumes that the variance equals the mean, the panel Poisson fixed-effects estimation is more flexible. It accounts for overdispersion and effectively handles sparse data. Additionally, by incorporating fixed effects, this model controls for unobserved regional heterogeneity, ensuring that differences across regions (such as socio-economic and ecological factors) do not distort the analysis[53]. This is particularly crucial when studying a large geographic area where baseline conflict risks may differ but remain relatively stable within each region over time. By controlling for these stable regional characteristics, we can more precisely assess the impact of droughts, floods, and other short-term climatic stresses on the likelihood of armed conflicts.

Using the panel Poisson fixed-effects model, we investigate how varying levels of droughts and floods influence the frequency of armed conflicts. The basic form of the model is:

$$Conflict_{it} = \exp\left(\beta Drought_{it} + \mu_i\right) + \varepsilon_{it} \quad (1)$$

$$Conflict_{it} = \exp(\beta Flood_{it} + \mu_i) + \varepsilon_{it} \quad (2)$$

where i represents the region and t represents the year. $Conflict\_it$ denotes the number of armed conflicts in region i during year t, corresponding to the frequency of armed conflicts. $Drought_{it}$ and $Flood_{it}$ represent the frequency of droughts and floods, respectively (we distinguish between different severities of droughts and floods by using *Normal* and *Extreme* categories). β is the coefficient. μ_i is the fixed effect, capturing the unobserved time-invariant heterogeneity across regions. ε_{it} is the error term.

We use the log-transformed coefficients from Poisson estimations to calculate Incidence Rate Ratio (IRR), providing a clear and rigorous measure of how climatic disruptions influence conflict likelihood. An IRR greater than 1 indicates that each incremental increase in the explanatory variable, such as an additional flood event, raises the expected conflict rate by the corresponding factor. By expressing regression results as relative risks, the IRR framework helps illustrate how repeated floods or droughts can intensify social unrest and drive conflict escalation.

Sample construction based on different buffer zones and different data processing methods

Though most analyses of hydrological climate change and conflict/security have focused on spatially constrained units (countries, regions, cities, communities), such impacts from both conflicts and climate may be transmitted spatially through population movements[54–56]. The buffer zones of varying radii are established for sample construction to capture these dynamics. The radius of the buffer zones in this study is determined based

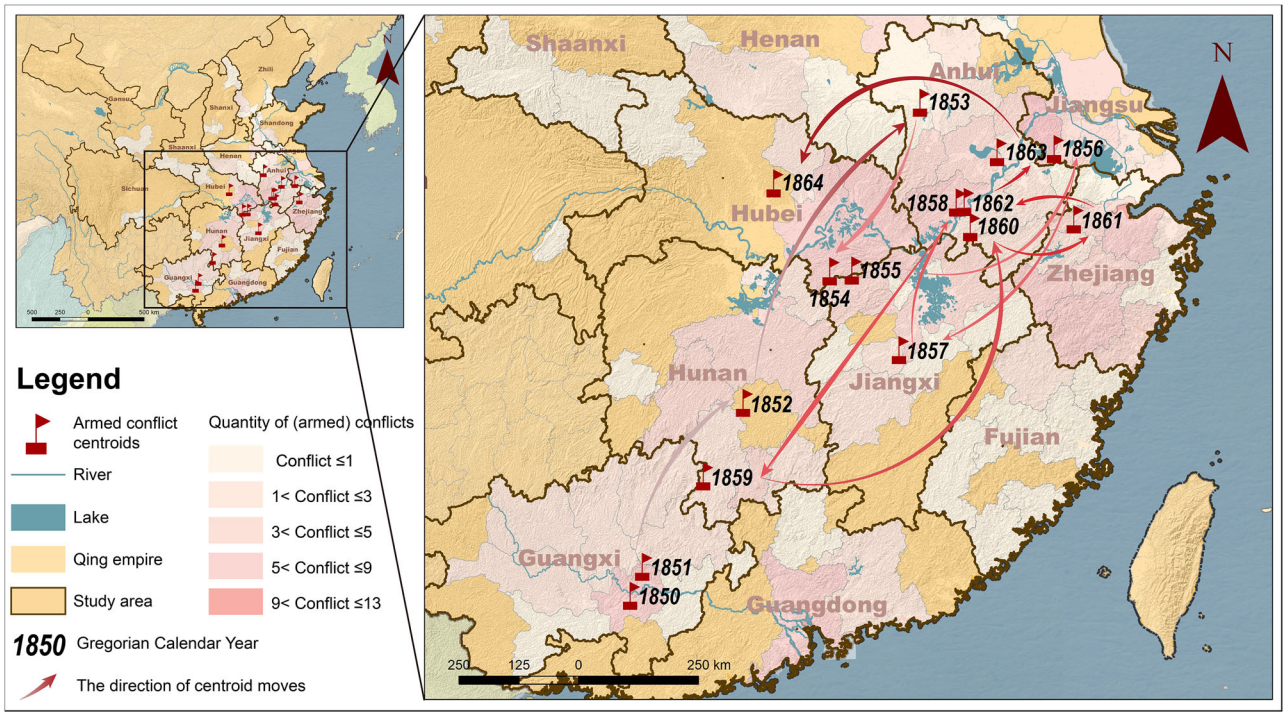

Fig. 2 | Annual centroids of the armed conflicts during the Taiping Rebellion. The centroids of armed conflicts for each year are shown. Red arrows indicate the direction of movement of these centroids over time. (Since the Taiping leaders began to gather in the late 1850, the 1850 uprising gathering location is added for reference).

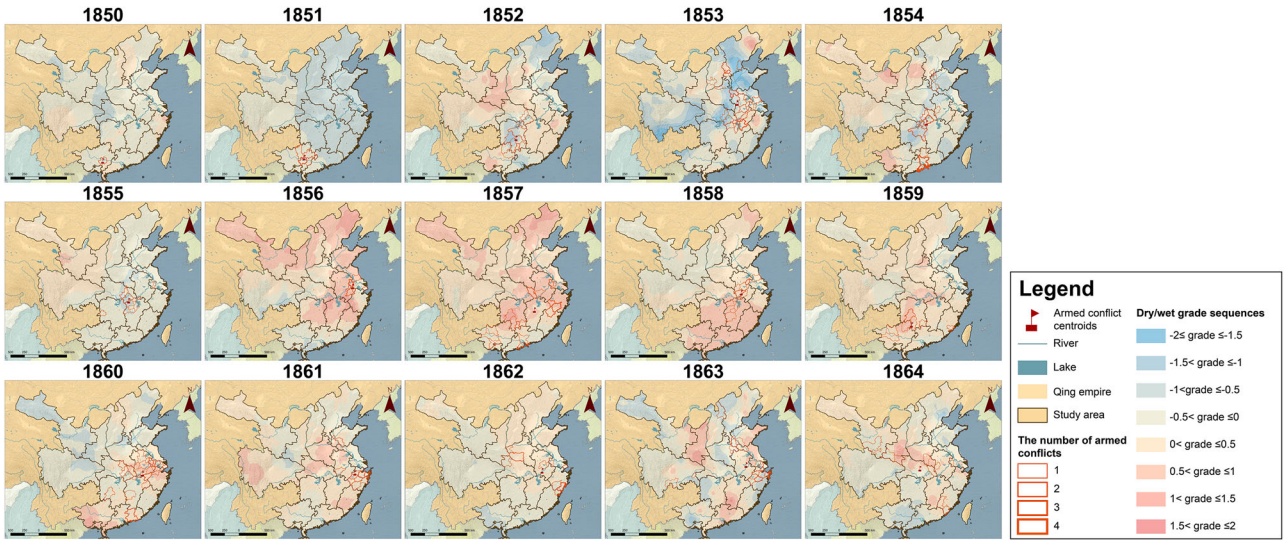

Fig. 3 | Annual wet-dry pattern and armed conflicts during the Taiping Rebellion (The pattern in 1850 is added for reference).

on the estimated walking speed of displaced refugees and the distances between various administrative units. While historical records often detail the dire conditions refugees face, they rarely provide explicit accounts of their movements during famines or disasters. However, certain historical facts allow us to infer the velocity of the refugee movement. Importantly, the speed at which refugees fled famine should not be equated with the walking pace of an average individual or a marching army. Disasters, like floods, frequently devastated villages, resulting in many displaced persons, including the elderly, children, and their belongings, who migrated in groups[49]. Furthermore, hunger and disease often slowed their progress significantly. A historical account from the *Records of the Three Kingdoms* describes Liu Bei's retreat to Jiangxia (modern-day Jiangxia District, Wuhan City, Hubei Province) alongside 100,000 residents of Fancheng (now Xiangyang City District, Hubei Province). This group could cover only 5 to 10 km per day[57]. Similarly, records from Dacheng Prefecture mention a traveler in winter, clad in a short coat and tattered shoes, who begged for alms on his journey home, managing to cover only 10 to 15 km per day[58]. Based on these accounts, it can be reasonably inferred that the average movement speed of displaced populations during such crises was approximately 10 km per day.

Regarding the distances between administrative units in Guangxi, Guilin, which served as the provincial capital during the Qing Dynasty, was approximately 70 km from its directly affiliated Yongning Prefecture. Other subordinate counties ranged from 40 to 125 km from the provincial capital[59]. As for the proximity between neighboring counties, Lingchuan County is located 2.5 km east of the Xin'an County border and 25 km southeast of Lingui County[59]. Given these distances, refugees could likely reach nearby villages or the closest counties within a day, neighboring

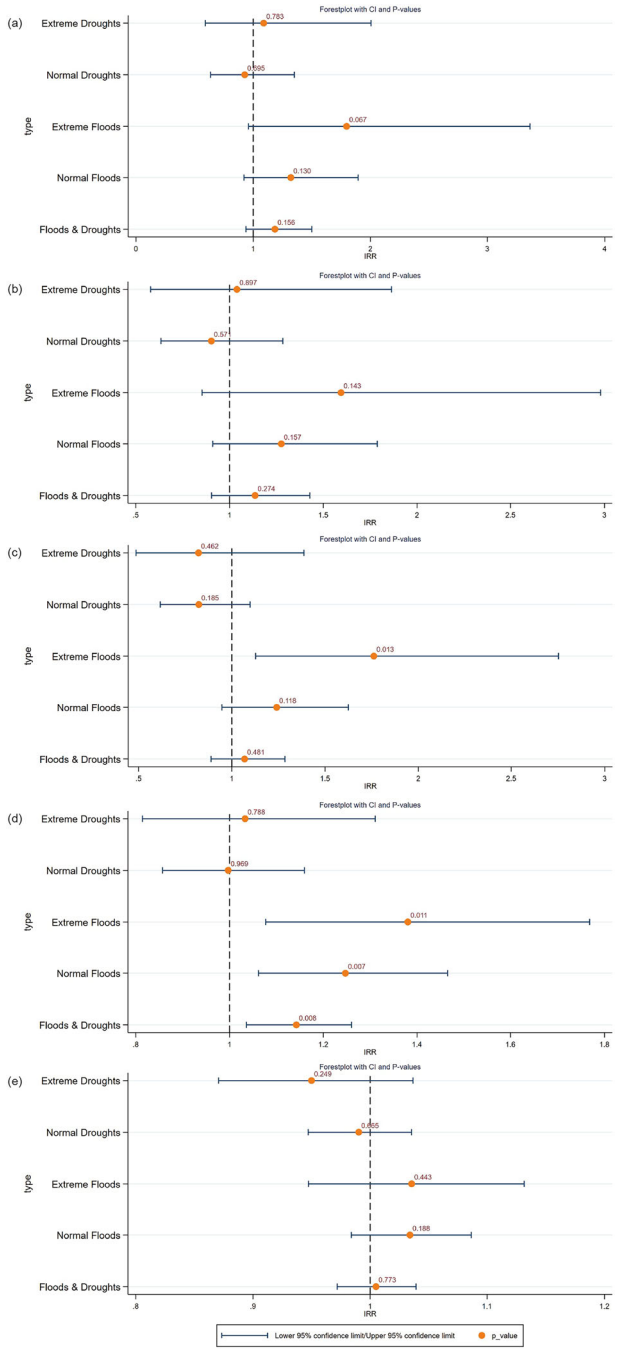

Fig. 4 | The impact of hydro-climatic extremes on armed conflicts during the Taiping Rebellion, with prefectures as the spatial analytical units. a Model without buffer zones; **b** Model with 10 km buffer zones; **c** Model with 25 km buffer zones; **d** Model with 50 km buffer zones; and **e** Model with 100 km buffer zones.

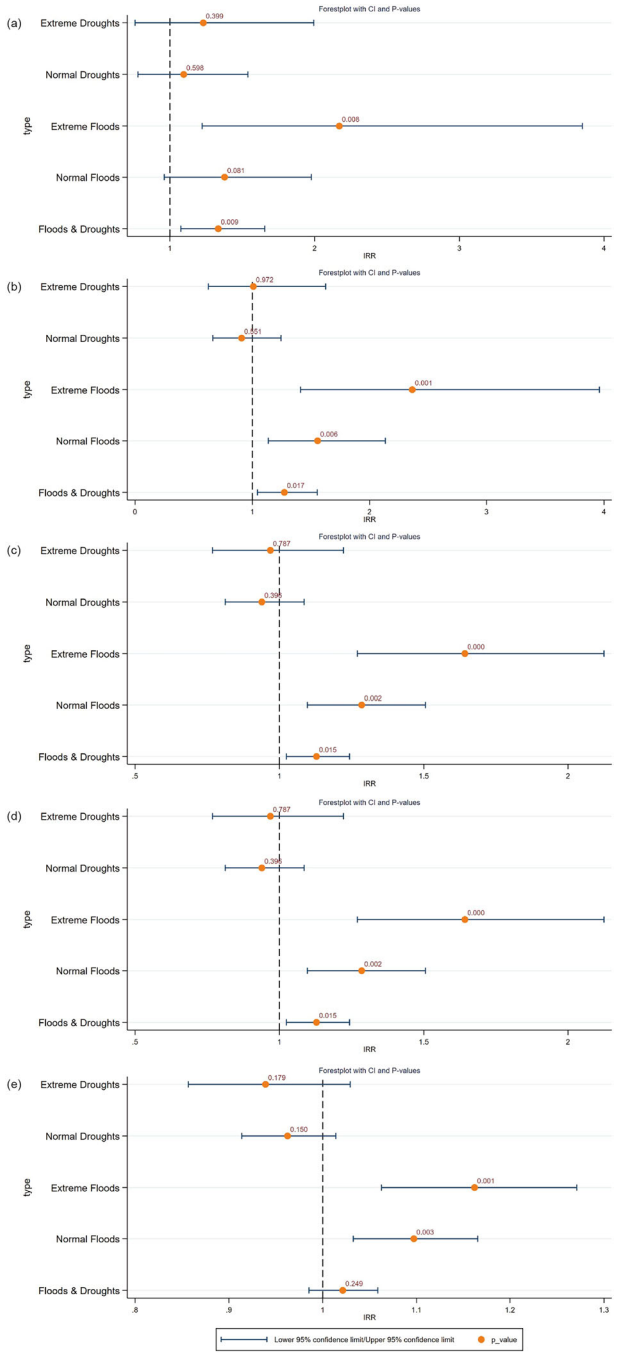

Fig. 5 | The impact of hydro-climatic extremes on armed conflicts during the Taiping Rebellion, with 100 km × 100 km grids as the spatial analytical units. a Model without buffer zones; **b** Model with 10 km buffer zones; **c** Model with 25 km buffer zones; **d** Model with 50 km buffer zones; and **e** Model with 100 km buffer zones.

counties within 2–3 days, and prefecture-level cities within 5–7 days, depending on their pace. Reaching the most distant administrative units, such as the provincial capital, would likely require over 10 days of travel.

In the sample construction of this study, we established buffer zones of the radii of 10 km, 25 km, 50 km, and 100 km to correspond with the distances from villages to counties, counties to adjacent counties, counties to prefectures, and prefectures to provincial capitals. These buffer zones allow us to examine the direction and extent of refugee mobility in response to varying levels of hydro-climatic extremes.

To ensure the reliability of our results and check for potential biases arising from the choice of spatial analytical units, we employed two methodological approaches in delineating the units. First, we delineated the units using the Qing administrative divisions (prefecture). However, we recognized that relying solely on this delineation could introduce spatial inconsistencies when analyzing historical events, as past and present administrative boundaries do not always align. To address this issue, we implemented a secondary approach using 100 km × 100 km grid cells, created with ArcGIS and clipped to the regions affected by the Taiping Rebellion. This grid-based framework ensures consistent spatial coverage and helps minimize distortions when administrative units vary greatly in size or shape. For example, in a large administrative region, a localized flood might be overlooked, while in a small unit, sparse data could lead to erratic

results. By comparing findings from both administrative division and grid-based methods, we ensure that our results are robust across different spatial analytical units, providing a more reliable foundation for analyzing the relationship between hydro-climatic extremes and armed conflicts.

Results

The overall effect of hydro-climatic extremes on armed conflicts

We calculated the Incidence Rate Ratio (IRR) by exponentiating the regression coefficients, which represent the multiplicative effect of a one-unit increase in an independent variable on the incidence rate of the dependent variable. This method helps to interpret the regression results better. An IRR greater than 1 indicates that the variable has a positive effect on the incidence of armed conflicts, while an IRR less than 1 suggests a negative effect. Figure 4 and Table S1 in Supplementary Information show that various hydro-climatic extremes are strongly correlated with armed conflicts when setting a 50 km buffer zone, with total hydro-climatic extremes (floods & droughts), normal floods, and extreme floods all positively correlated with armed conflicts. An increase of 1 unit in total hydro-climatic extremes (floods & droughts), normal floods, and extreme floods corresponded to an increase in armed conflicts by 14.3% ($p < 0.01$), 24.7% ($p < 0.01$), and 38.0% ($p < 0.05$), respectively. Among the different hydro-climatic extremes, the strongest correlation was found between extreme floods and armed conflicts. With no buffer, 25 km buffer, and 50 km buffer, an increase of 1 unit in extreme floods corresponded to an increase in the incidence of armed conflicts by 79.7% ($p < 0.1$), 76.2% ($p < 0.05$), and 38.0% ($p < 0.05$), respectively. Overall, the value of IRR decreases with the expansion of the buffer zone, which implies that the impact of hydro-climatic extremes decreases with the expansion of the buffer zone.

Figure 5 and Table S2 in Supplementary Information reveal that when 100 km × 100 km grids are used as the spatial analytical units, the effects of hydro-climatic extremes (floods & droughts) on armed conflicts become more significant than when prefectures are used as spatial units. Total hydro-climatic extremes (flood & drought) strongly correlate with armed conflicts across all buffer zone settings (no buffer, 10 km, 25 km, and 50 km). However, the IRR values decrease as the buffer zone expands, reinforcing the trend observed in the previous analysis. As for normal floods and extreme floods, their effects are the greatest when setting a 10 km buffer zone: the incidence of armed conflicts corresponds to an increase of 55.7% ($p < 0.01$) and 136.4% ($p < 0.01$) for normal floods and extreme floods respectively with an increase of 1 unit and then decreases with the buffer zone expansion. These two hydro-climatic extremes have the same effect on armed conflicts in 25 km and 50 km buffer zones. Compared to floods, droughts are not significantly correlated with armed conflicts under both data treatments.

The effect of hydro-climatic extremes on armed conflicts in different time segments

Since Fig. 3 shows that different wet and dry patterns are exhibited in the first half (1851–1857) and the second half (1858–1864) of the Taiping Rebellion, we performed time-segmented sample regression on the Taiping Rebellion data to test the robustness of our findings presented in the previous section. The results show that hydro-climatic extremes, especially floods, had a positive impact on the incidence of armed conflicts in both the first half and the second half of the Taiping Rebellion, regardless of which spatial analytical unit was used (Tables S3–S6 in Supplementary Information).

The cumulative effect of hydro-climatic extremes on armed conflicts

To further explore the cumulative impacts of hydro-climatic extremes during the Taiping Rebellion, we conducted a cross-sectional Poisson model. The related results are presented in Tables S7 and S8 in Supplementary Information. Hydro-climatic extremes are strongly and positively correlated with armed conflicts at all buffer zone ranges, whether using prefectures or 100 km × 100 km grids as the spatial analytical units. Taking the data processed by grids as an example, hydro-climatic extremes have the most significant impact on armed conflicts when no buffer zones are set: for every unit increase in total hydro-climatic extremes (floods & and droughts), the incidence of armed conflicts increases by 12.8%, 23.0%, 50.9%, 30.2%, and 153.2% for normal floods, extreme floods, normal droughts, and extreme droughts, respectively. It is important to note that while droughts are not correlated with armed conflicts in the panel Poisson fixed-effects estimation, their cumulative effects on armed conflicts appear to be more pronounced than those of floods. This suggests that droughts do not have an immediate impact on conflicts within the same year. However, prolonged droughts do have a significant effect on the incidence of armed conflicts over time.

Discussion

Hydrological and climatic variability affects human societies primarily through intermediary socio-economic factors, particularly in agrarian communities where agricultural production and governance are key determinants of social stability. This relationship has been well-documented in previous studies at the global level[60–63]. Although our statistical models do not include these intermediary factors explicitly, their crucial role in mediating the relationship between climate events and conflicts cannot be neglected. Therefore, our findings are interpreted in light of historical evidence and contextual information related to these factors.

Previous studies show that the intensity of droughts and floods and their subsequent impacts on societies vary across regions[14,60,64–66]. The results of this study indicate that floods have a more pronounced impact on armed conflicts than droughts, with the severity of flooding positively correlating with the likelihood of armed conflicts. Droughts, on the other hand, only impact armed conflicts if they are prolonged and continuous. This may be attributed to how floods and droughts affect agricultural output and economic activities. Both extreme floods and droughts result in significant agricultural losses; however, their impacts differ in nature and immediacy. Floods tend to cause sudden and severe destruction of farmland and settlements[67], often forcing affected individuals to abandon their homes and relocate to nearby areas. In contrast, droughts develop more gradually, affecting agricultural production over a longer period and are generally easier to manage[67]. In the short term, the southern regions in China, where the Taiping Rebellion predominantly occurred, were better equipped to cope with drought due to their dense river networks and extensive water infrastructure[68,69], which helped to alleviate water shortages. Furthermore, the widespread cultivation of drought-resistant crops such as sweet potatoes and maize likely softened the impact of drought on agricultural output[12]. Hence, droughts had a comparatively smaller effect on food production than floods[67], and were less likely to cause large-scale displacement to nearby cities in the short term.

This study employs two spatial data frameworks—Qing administrative divisions and 100 km × 100 km grids—to examine the relationship between hydro-climatic disasters and civil conflicts during the Taiping Rebellion. Our regression results are more significant for 100 km × 100 km grids as the spatial analytical units. This may be because hydro-climatic extremes do not evolve along administrative divisions, and the use of grids captures their free-dispersing effects better than the use of administrative divisions in the data treatment. The findings from both spatial frameworks consistently demonstrate that floods significantly influence the emergence of armed conflicts in neighboring regions, supporting our hypothesis that flood-induced displacement contributes to civil unrest in adjacent areas. This finding aligns with historical evidence. For instance, in 1848, severe flooding struck Changsha City in Hunan Province, displacing hundreds of thousands of people. The resulting influx of refugees into the city led to widespread theft and robbery both within the city and in surrounding areas[49]. Similarly, in the summer of 1853, flooding in Gaoyou, Jiangsu Province, drove large numbers of refugees into Yangzhou, causing grain prices to spike and triggering incidents of small-scale grain looting[70]. A comparable situation occurred in Huzhou, Zhejiang Province, in 1860, when conflict erupted between flood refugees and local farmers over farmland. The government responded by deploying troops to suppress the violence[71].

Moreover, the extent to which floods impact armed conflicts appears to depend on the mobility of displaced populations, as measured by the defined buffer zones. Our regression results indicate that in 100 km × 100 km grids, the influence of both normal and extreme floods on armed conflicts increases when the buffer zone is set in our statistical models, peaking at a distance of 10 km, and then gradually declines. In contrast, within a broader 100 km buffer zone, there appears to be little correlation between flood events and conflict incidence. This pattern reaffirms that floods trigger conflicts primarily through the displacement and migration of affected populations. Flood victims are more likely to relocate to nearby counties rather than distant major cities, thereby increasing the likelihood of conflict in areas closer to the origin of the disaster. This may be due to two different factors. One is that catastrophic floods devastate homes and farmland, leading to famine and poverty, which in turn decreases the mobility of refugees. In unison, local authorities often restricted refugee access to major administrative centers or cities to prevent looting, theft, and potential uprisings, particularly during large-scale displacements caused by extreme floods. This strategy was particularly evident in the capital, Beijing, where Qing Dynasty authorities set up border checkpoints to prevent refugees from entering the city[72]. In unison, the government also set up congee kitchens and shelters on the outskirts of the capital and in nearby counties and cities to support some of the displaced population[73]. However, these measures shifted the burden to lower-level administrative units, which faced increased pressure to accommodate refugees, heightening the risk of armed conflicts.

The Taiping Rebellion emerged against hydro-climatic extremes that intensified already fragile population-environment dynamics. Before the rebellion, the Guangxi region suffered from prolonged floods and droughts, which devastated agricultural land and displaced large numbers of peasants[74,75]. Many of these landless peasants moved to urban centers such as Nanning and Guilin in search of livelihoods[76,77]. However, the influx of refugees into cities with already limited resources worsened food shortages, drove up prices, and fueled tensions between local residents and newcomers[39,74,75]. For instance, in Wuzhou Prefecture, the drought of 1845 triggered a sharp rise in refugee numbers. Competition between refugees and locals over access to water escalated into violent riots[78]. In 1849, another severe drought struck Guangxi. In response, desperate refugees looted food supplies in Liuzhou and Guilin and even attacked local authorities for releasing grain from government storage[77,79].

The Qing government's response to the growing unrest was widely regarded as a failure. Instead of addressing the root causes of the crisis, authorities suppressed the refugees and continued to impose taxes even during times of famine[80]. In stark contrast, the Taiping Heavenly Kingdom's platform, promising shared land and food (plowing together, eating together), resonated strongly with the starving and landless displaced population[81]. Capitalizing on this discontent, rebel leader Hong Xiuquan distributed food to refugees, winning over many followers. As local governance collapsed and the appeal of land redistribution grew, displaced people gradually united to form the foundation of a militia force[82]. By the time of the Jintian Uprising in 1851, over half of the initial 20,000 participants were displaced peasants who had lost their homes due to hydro-climatic extremes[83]. This was recorded in the *Records of Guiping County* that most of the participants were displaced persons with "hungry faces"[77]. The Taiping Rebellion emerged out of these challenging climatic and socio-economic conditions.

In the case of the Taiping Rebellion, the process from the outbreak of hydro-climatic extremes to the armed conflicts also involved the migration of refugees, the failure of local governance, and the collapse of the economy. The chaotic migration and the influx of impoverished and homeless refugees caused environmental overload in the receiving regions, which triggered a series of negative socio-economic consequences. Nowadays, there are still many underdeveloped countries whose socio-economic settings are very similar to the historical agrarian societies (like the Qing dynasty), facing the short-term challenge of not being able to enhance the carrying capacity of the environment (e.g., increase crop yields)[84] and enhance local governance capacity[85] in the short term. It is necessary to consider the scale of climate refugee migration, their migration capacity, and strategies to manage the risk of conflicts. Climate refugee migration is now more cross-border (e.g., transnational movements triggered by droughts in sub-Saharan Africa[86,87]). However, the absence of a targeted protection framework in international law (climate refugees are not covered by *The 1951 Refugee Convention*) increases the risk that those who cross borders will have to move through informal channels[88,89]. All of these call for the international community to expand the legal framework for climate refugees and to plan for orderly migration to reduce climate change-triggered conflicts.

This study provides a nuanced examination of the impact of hydro-climatic extremes on violent conflicts during the Taiping Rebellion, offering new insights into the spatial dynamics of climate-induced social unrest. By employing the panel Poisson fixed-effects estimation, we demonstrate that floods had a more significant influence on the outbreak of armed conflicts than droughts. The intensity of floods positively correlates with conflict frequency, a finding consistently supported by both prefecture and 100 km × 100 km grid spatial data.

Our analysis shows that the spillover effects of hydro-climatic extremes, primarily driven by refugee migration, vary with distance from the disaster's origin. Floods are more likely to trigger conflicts in nearby smaller, sub-regional cities rather than in distant, inter-provincial towns. The impact of both normal and extreme floods on armed conflicts decreases as the buffer zone expands, echoing the refugee mobility during the late Qing Dynasty.

Moving beyond the static analysis of the climate-conflict nexus, this study advances our understanding of how spatial and environmental factors interact to shape social stability. The findings underscore the importance of considering spatial heterogeneity and migration dynamics when assessing the broader societal impacts of climate extremes. In doing so, this research illuminates the complex mechanisms by which climate variability can exacerbate underlying social tensions, offering valuable lessons for contemporary discussions on climate change and violent conflicts.

Data availability

The datasets generated and analyzed during the current study are available from the corresponding author upon reasonable request. The data analysis in this study can be obtained from the corresponding author upon reasonable request.

Received: 18 November 2024; Accepted: 7 May 2025;
Published online: 22 May 2025

References

1. Wang, Q. et al. Quantifying the influence of climate variability on armed conflict in Africa, 2000–2015. *Environ. Dev. Sustain.* **25**, 9289–9306 (2023).
2. Schleussner, C.-F., Donges, J. F., Donner, R. V. & Schellnhuber, H. J. Armed-conflict risks enhanced by climate-related disasters in ethnically fractionalized countries. *Proc. Natl Acad. Sci. USA* **113**, 9216–9221 (2016).
3. von Uexkull, N., Croicu, M., Fjelde, H. & Buhaug, H. Civil conflict sensitivity to growing-season drought. *Proc. Natl Acad. Sci. USA* **113**, 12391–12396 (2016).
4. Jones, B. T., Mattiacci, E. & Braumoeller, B. F. Food scarcity and state vulnerability: unpacking the link between climate variability and violent unrest. *J. Peace Res.* **54**, 335–350 (2017).
5. Mach, K. J. et al. Climate as a risk factor for armed conflict. *Nature* **571**, 193–197 (2019).
6. Mack, E. A. et al. Conflict and its relationship to climate variability in Sub-Saharan Africa. *Sci. Total Environ.* **775**, 145646 (2021).
7. Parenti, C. Flower of war: an environmental history of opium poppy in Afghanistan. *SAIS Rev. Int. Aff.* **35**, 183–200 (2015).
8. Gleick, P. H. Water, drought, climate change, and conflict in Syria. *Weather Clim Soc* **6**, 331–340 (2014).

9. Kelley, C. P., Mohtadi, S., Cane, M. A., Seager, R. & Kushnir, Y. Climate change in the Fertile Crescent and implications of the recent Syrian drought. *Proc. Natl Acad. Sci. USA* **112**, 3241–3246 (2015).
10. Wischnath, G. & Buhaug, H. On climate variability and civil war in Asia. *Clim. Change* **122**, 709–721 (2014).
11. Xie, X. et al. Exploring the direct and indirect impacts of climate variability on armed conflict in South Asia. *iScience* **25**, https://doi.org/10.1016/j.isci.2022.105258 (2022).
12. Jia, R. Weather shocks, sweet potatoes and peasant revolts in historical China. *Econ. J.* **124**, 92–118 (2014).
13. Kung, J. K. & Ma, C. Can cultural norms reduce conflicts? Confucianism and peasant rebellions in Qing China. *J. Dev. Econ.* **111**, 132–149 (2014).
14. Lee, H. F., Zhang, D. D., Pei, Q., Jia, X. & Yue, R. P. H. Quantitative analysis of the impact of droughts and floods on internal wars in China over the last 500 years. *Sci. China Earth Sci.* **60**, 2078–2088 (2017).
15. Zhang, D. D. et al. Climatic change, wars and dynastic cycles in China over the last millennium. *Clim. Change* **76**, 459–477 (2006).
16. Fagan, B. *The Little Ice Age: How Climate Made History 1300-1850* (Basic Books, 2000).
17. Ge, Q. *Climatic Variations in the Chinese Past Dynasties* (Science Press, 2011).
18. Hinsch, B. Climatic change and history in China. *J. Asian Hist.* **22**, 131–159 (1988).
19. Zhang, D., Jim, C., Lin, C., He, Y. & Lee, F. Climate change, social unrest and dynastic transition in ancient China. *Chin. Sci. Bull.* **50**, 137–144 (2005).
20. Zheng, J. et al. How climate change impacted the collapse of the Ming dynasty. *Clim. Change* **127**, 169–182 (2014).
21. Büntgen, U. et al. 2500 years of European climate variability and human susceptibility. *Science* **331**, 578–582 (2011).
22. Douglas, P. M. J. et al. Drought, agricultural adaptation, and sociopolitical collapse in the Maya Lowlands. *Proc. Natl Acad. Sci. USA* **112**, 5607–5612 (2015).
23. Kennett, D. J. et al. Drought-induced civil conflict among the ancient Maya. *Nat. Commun.* **13**, 3911 (2022).
24. Douglas, P. M. J., Demarest, A. A., Brenner, M. & Canuto, M. A. Impacts of climate change on the collapse of lowland Maya civilization. *Annu. Rev. Earth Planet. Sci.* **44**, 613–645 (2016).
25. Hsiang, S. M., Meng, K. C. & Cane, M. A. Civil conflicts are associated with the global climate. *Nature* **476**, 438–441 (2011).
26. Fang, X. & Su, Y. The relationship between famine, peasant uprisings and climate change in China over the past 2000 years. in *The Social Impacts of Climate Change in China over the Past 2000 Years* (eds Fang, X. et al.) 195–213 (Springer Nature, 2024),
27. Cramer, C. & Richards, P. Violence and war in Agrarian perspective. *J. Agrar. Change* **11**, 277–297 (2011).
28. Paige, J. M. *Agrarian Revolution: Social Movements and Export Agriculture in the Underdeveloped World* (The Free Press, 1976).
29. Fan, K. Climate change and Chinese history: a review of trends, topics, and methods. *WIREs Clim. Change* **6**, 225–238 (2015).
30. Zhang, Z. et al. Periodic climate cooling enhanced natural disasters and wars in China during AD 10–1900. *Proc. R. Soc. B Biol. Sci.* **277**, 3745–3753 (2010).
31. Daye, Z. *The World of a Tiny Insect: A Memoir of the Taiping Rebellion and Its Aftermath* (University of Washington Press, 2013).
32. Xu, L. C. & Yang, L. *Stationary Bandits, State Capacity, and the Malthusian Transition: The Lasting Impact of the Taiping Rebellion,* Policy Research Working Paper No. WPS 8620, http://documents.worldbank.org/curated/en/970791540230641485 (World Bank Group, 2018).
33. Kilcourse, C. Review of The World of a Tiny Insect: a memoir of the Taiping Rebellion and its aftermath, Zhang Daye, translated by Xiaofei Tian. *J. Am. Orient. Soc.* **136**, 156–158 (2016).
34. Frey, K. Taiping Rebellion. In *The Palgrave Encyclopedia of Imperialism and Anti-Imperialism* (eds Ness, I. & Cope Z.) 2587–2595 (Springer International Publishing, 2021).
35. Li, B. The Daoguang Depression and the 1823 flood—economic decline, climatic cataclysm and the nineteenth-century crisis in Songjiang. *J. Soc. Sci.* **6**, 173–178 (2007).
36. Ge, J. *Population and China's Modernization: Since 1850* (Xuelin Press, 1999).
37. Hao, Z., Xiong, D. & Zheng, J. Flood disasters and social resilience during the decline of the Qing Dynasty: case studies of 1823 and 1849. *Hydrol. Process.* **35**, e14295 (2021).
38. Ge, Q. S. & Wang, W. Q. Population pressure, climate change and taiping rebellion. *Geogr. Res.* **14**, 32–41 (1995).
39. Xie, Q. & Hu, W. *Guang Xi Tong Zhi [Guangxi Province Gazetteer]* (Guangxi People's Publishing House, 1988).
40. Xiao, L., Ye, Y. & Wei, B. Revolts frequency during 1644–1911 in North China Plain and its relationship with climate. *Adv. Clim. Change Res.* **2**, 218–224 (2011).
41. Editorial Committee of Chinese Military History. *Zhongguo Junshishi [Tabulation of Wars in Historical China] (II)* (Liberation Army Publishing House, 1985).
42. Chinese National Meteorological Administration. *Zhongguo Jin Wubainian Hanlao Fenbu Tuji [Yearly Charts of Dryness/Wetness in China for the Last 500-year Period]* (Chinese Cartographic Publishing House, 1981).
43. Beijing Taiping Rebellion Historical Research Society. *History of the Taiping Rebellion-Second Volume* (Zhonghua Book Company, 1893).
44. Feuerwerker, A. & Chiang, S. The Nien Rebellion. *Harv. J. Asiat. Stud.* **19**, 165 (1956).
45. Reichen, L. et al. A decade of cold Eurasian winters reconstructed for the early 19th century. *Nat. Commun.* **13**, 2116 (2022).
46. Barriendos, J., Hernández, M., Gil-Guirado, S., Olcina Cantos, J. & Barriendos, M. Droughts of the early 19th century (1790–1830) in the northeastern Iberian Peninsula: integration of historical and instrumental data for high-resolution reconstructions of extreme events. *Climate* **20**, 2595–2616 (2024).
47. Wei, Z. & Li, B. Relationship between Famine and climatic disasters in China during the Qing Dynasty. *Weather Clim Soc* **16**, 171–183 (2024).
48. Klein, J., Nash, D. J., Pribyl, K., Endfield, G. H. & Hannaford, M. Climate, conflict and society: changing responses to weather extremes in nineteenth century Zululand. *Environ. Hist.* **24**, 377–401 (2018).
49. Deng, Y. *History of Chinese Famine Relief* (The Commercial Press, 1989).
50. Rodell, M. & Li, B. Changing intensity of hydroclimatic extreme events revealed by GRACE and GRACE-FO. *Nat. Water* **1**, 241–248 (2023).
51. Bai, H., Dong, A. & Zheng, G. (eds) *Zhongguo xi bei di qu jin wu bai nian han lao fen bu tu ji: 1470-2008 [Yearly Charts of Dryness/Wetness in North Western China for the Last 500-year Period (1470–2008)] 1st edn* (China Meteorological Press, 2010).
52. Lee, H. F. Internal wars in history: triggered by natural disasters or socio-ecological catastrophes? *Holocene* **28**, 1071–1081 (2018).
53. Allison, P. D. *Fixed Effects Regression Models* (Sage, 2009).
54. Kallis, G. & Zografos, C. Hydro-climatic change, conflict and security. *Clim. Change* **123**, 69–82 (2014).
55. Lee, H. F. & Qiang, W. Climatic extremes, violent conflicts, and population change in China in 1741–1910: an investigation using spatial econometrics. *Anthropocene* **41**, 100372 (2023).
56. Malaekeh, S., Shiva, L. & Safaie, A. Climate change impacts on agriculture: do spatial spillovers matter? EGU22-4016. https://doi.org/10.5194/egusphere-egu22-4016 (2022).
57. Chen, S. *Records of the Three Kingdoms* (Zhonghua shu ju, 2015).
58. Zhao, B. *Local Gazetteer of Dacheng County* 1st edn (Huaxia Publishing House, 1995).

59. Su, Z. *Guang Xi Tong Zhi Ji Yao* [*Guangxi Gazetter Compilation in Guangxu Period*]. http://x.wenjinguan.com/default.aspx (1890).
60. Fjelde, H. & von Uexkull, N. Climate triggers: rainfall anomalies, vulnerability and communal conflict in Sub-Saharan Africa. *Political Geogr.* **31**, 444–453 (2012).
61. Hendrix, C. S. & Salehyan, I. Climate change, rainfall, and social conflict in Africa. *J. Peace Res.* **49**, 35–50 (2012).
62. Carleton, T. A. & Hsiang, S. M. Social and economic impacts of climate. *Science* **353**, aad9837 (2016).
63. Zhang, D., Li, J., Ji, Q. & Managi, S. Climate variations, culture and economic behaviour of Chinese households. *Clim. Change* **167**, 9 (2021).
64. Bai, Y. & Kung, J. K. Climate shocks and Sino-nomadic conflict. *Rev. Econ. Stat.* **93**, 970–981 (2011).
65. Chaney, E. Revolt on the Nile: economic shocks, religion, and political power. *Econometrica* **81**, 2033–2053 (2013).
66. Hsiang, S. M., Burke, M. & Miguel, E. Quantifying the influence of climate on human conflict. *Science* **341**, 1235367 (2013).
67. Lin, K.-H. E., Wang, P. K., Pai, P.-L., Lin, Y.-S. & Wang, C.-W. Historical droughts in the Qing dynasty (1644–1911) of China. *Climate* **16**, 911–931 (2020).
68. Liu, B. et al. Earliest hydraulic enterprise in China, 5,100 years ago. *Proc. Natl Acad. Sci. USA* **114**, 13637–13642 (2017).
69. Willmott, W. E. Dujiangyan: irrigation and society in Sichuan, China. *Aust. J. Chin. Aff.* **22**, 143–153 (1989).
70. Wen, Q. & Zong, S. L. *Veritable Records of the Qing Dynasty in Xianfeng Period*, *97* (Zhonghua Book Company, 1985).
71. Ge, J. et al. (eds) *Zhongguo yi min shi (China's Migration History), 6* 1st edn (Fudan University Press, 2022).
72. Xiao, L., Fang, X., Zhang, Y., Ye, Y. & Huang, H. Multi-stage evolution of social response to flood/drought in the North China Plain during 1644–1911. *Reg. Environ. Change* **14**, 583–595 (2014).
73. Fuller, P. *Famine Relief in Warlord China* (Brill, 2021).
74. Li, D. Q. & Shi, C. *Veritable Records of the Qing Dynasty in Daoguang Period* (Zhonghua Book Company, 1985).
75. Zhao, E. & Shi, Q. *Draft History of Qing* 40–44 (Zhonghua Book Company, 1977).
76. Su, S. *Nan Ning Fu Zhi* [*Nanning City Gazetteer*]. http://x.wenjinguan.com/default.aspx (1909).
77. Ping, G. & Zhi, X. *Guiping County Gazetteer* (Chengwen Publishing Company, 1968).
78. Zhou, W. & Zhi, F. *Wuzhou City Gazetteer* (Chengwen Publishing Company, 1976).
79. He, W., Xie, S., Liu, C. & Zhi, X. *Liucheng County Gazetteer* (Chengwen Publishing Company, 1967).
80. Platt, S. R. *Autumn in the Heavenly Kingdom: China, the West, and the Epic Story of the Taiping Civil War* (Knopf Doubleday Publishing Group, 2012).
81. Kikuchi, H. *Guangxi yimin shehui yu taiping tianguo (Immigrant society in Guangxi and the Taiping Heavenly Kingdom)* (Fûkyôsha, 1998).
82. Jian, Y. *The Taiping Revolutionary Movement* (New Haven, 1973).
83. Luo, E. *Tai ping tian guo shi (History of Taiping Heavenly Kingdom)* (Zhonghua Book Company, 1991).
84. FAO, ECA, AUC. *Africa—Regional Overview of Food Security and Nutrition 2021* (FAO, 2021).
85. Fagbemi, F., Nzeribe, G. E., Osinubi, T. T. & Asongu, S. Interconnections between governance and socioeconomic conditions: understanding the challenges in sub-Saharan Africa. *Reg. Sustain.* **2**, 337–348 (2021).
86. United Nations Environment Programme (UNEP). Livelihood Security: Climate Change, Migration and Conflict in the Sahel. (United Nations Environment Programme, 2011).
87. Tesfaye, B. *Climate Change and Conflict in the Sahel*. Discussion Paper Series on Managing Global Disorder No. 11 (The Council on Foreign Relations, 2022).
88. Mcadam, J. Climate change-related movement and International Human Rights Law: the role of complementary protection. in *Climate Change, Forced Migration, and International Law* (ed. McAdam, J.) (Oxford University Press, 2012).
89. Mcadam, J. The relevance of International Refugee Law. in *Climate Change, Forced Migration, and International Law* (ed. McAdam, J.) (Oxford University Press, 2012).

Acknowledgements

This research is supported by the Humanities and Social Sciences Prestigious Fellowship Scheme (34000323), University Grants Committee, Hong Kong.

Author contributions

H.F.L.: conceptualization and validation. W.W.Q.: data curation and software. H.F.L. and W.W.Q.: methodology. C.J. and H.F.L.: writing—original draft preparation. C.J. and H.F.L.: writing—review and editing. H.F.L.: supervision. All authors have read and agreed to the published version of the manuscript.

Competing interests

The authors declare no competing interests.

Additional information

Supplementary information The online version contains supplementary material available at https://doi.org/10.1038/s40494-025-01779-8.

Correspondence and requests for materials should be addressed to Harry F. Lee.